

Back-Hopping in Spin-Transfer-Torque Devices: Possible Origin and Countermeasures

Claas Abert,^{1,*} Hossein Sepehri-Amin,² Florian Bruckner,¹ Christoph Vogler,³ Masamitsu Hayashi,^{2,4} and Dieter Suess¹

¹*Christian Doppler Laboratory of Advanced Magnetic Sensing and Materials, Faculty of Physics, University of Vienna, Vienna 1090, Austria*

²*National Institute for Materials Science, Tsukuba 305-0047, Japan*

³*Faculty of Physics, University of Vienna, Vienna 1090, Austria*

⁴*Department of Physics, The University of Tokyo, Bunkyo, Tokyo 113-0033, Japan*

 (Received 9 June 2017; revised manuscript received 4 December 2017; published 8 May 2018)

The effect of undesirable high-frequency free-layer switching in magnetic multilayer systems, referred to as back-hopping, is investigated by means of the spin-diffusion model. A possible origin of the back-hopping effect is found to be the destabilization of the pinned layer, which leads to the perpetual switching of both layers. While the presented mechanism is not claimed to be the only possible reason for back-hopping, we show that it is a fundamental effect that will occur in any spin-transfer-torque device when exceeding a critical current. The influence of different material parameters on the critical switching currents for the free and pinned layer is obtained by micromagnetic simulations. The spin-diffusion model enables an accurate description of the torque on both layers, depending on various material parameters. It is found that the choice of a free-layer material with low polarization β and saturation magnetization M_s and a pinned-layer material with high β and M_s leads to a low free-layer critical current and a high pinned-layer critical current and hence reduces the likelihood of back-hopping. While back-hopping has been observed in various types of devices, there are only a few experiments that exhibit this effect in perpendicularly magnetized systems. However, our simulations suggest that the described effect will also gain importance in perpendicular systems due to the loss of pinned-layer anisotropy for decreasing device sizes.

DOI: [10.1103/PhysRevApplied.9.054010](https://doi.org/10.1103/PhysRevApplied.9.054010)

I. INTRODUCTION

Spin-transfer torque (STT) in magnetic multilayers has gained a lot of interest in recent years due to possible applications in alternative storage devices. A prominent candidate for such a STT magnetic random-access memory (MRAM) is a trilayer system consisting of two magnetic layers separated by a nonmagnetic layer [1–3]. If an electric current passes through this system, one of the magnetic layers acts as a spin polarizer. The other layer is subject to the spin torque exerted by the spin-polarized electrons. Depending on the sign of the electric current, the magnetization of this free layer can be switched in either direction. Since the spin-torque coupling is bidirectional, the spin-polarizing layer, also referred to as the pinned layer, is usually constructed to be very stiff in order to prevent switching.

The spacer layer between the magnetic layers can be either a conductor or an insulator. In case of an insulator, the spin-polarized electrons must tunnel through the spacer in order to exert a torque on the free-layer magnetization. The magnetization in the magnetic layers can be either in plane or out of plane. In the case of in-plane magnetization,

the pinned layer is mainly stabilized by its thickness, which leads to a high shape anisotropy. In the case of out-of-plane magnetization, the pinned layer is a magnetic multilayer system with high uniaxial anisotropy.

It has been observed in different in-plane devices that the free-layer magnetization might be unstable after switching. This back-hopping effect happens after overcoming the critical switching current and results in fast switching of the free layer [4–7]. Different explanations for this effect have been proposed [8,9]. One possible explanation is the destabilization of the pinned layer that causes the perpetual switching of both the free layer and the pinned layer [10]. Similar switching mechanics in a multilayer structure with a single pinned layer and two free layers were investigated in Ref. [11]. In this work, we investigate the switching in a classical perpendicular STT-MRAM device with pinned and free layers by means of micromagnetic simulations coupled to a spin-diffusion model. This technique allows us to study the effects of various material parameters on the back-hopping effect.

II. MODEL

According to the micromagnetic model, the magnetization dynamics are governed by the Landau-Lifshitz-Gilbert (LLG) equation

*claas.abert@univie.ac.at

$$\frac{\partial \mathbf{m}}{\partial t} = -\gamma \mathbf{m} \times \mathbf{h}_{\text{eff}} + \alpha \mathbf{m} \times \frac{\partial \mathbf{m}}{\partial t}, \quad (1)$$

where \mathbf{m} is the normalized magnetization, γ is the gyro-magnetic ratio, α is the Gilbert damping, and \mathbf{h}_{eff} is the effective field that usually contains the demagnetization field and the exchange field, as well as other contributions depending on the problem setting. A popular extension to the LLG for the description of spin-transfer torque is the model of Slonczewski [12] that complements the right-hand side of Eq. (1) with the torque term

$$\mathbf{T} = \eta_{\text{damp}}(\theta) J_e \mathbf{m} \times (\mathbf{m} \times \mathbf{M}) + \eta_{\text{field}}(\theta) J_e \mathbf{m} \times \mathbf{M}, \quad (2)$$

with \mathbf{M} being the pinned-layer magnetization, J_e being the signed electric current density (a positive sign means electrons are flowing from the pinned to the free layer), and η_{damp} and η_{field} being the angular dependence of the dampinglike and fieldlike torque, respectively; see, e.g., Ref. [13]. Here, θ is the angle between the magnetization \mathbf{m} and \mathbf{M} . This widely used model has a number of drawbacks for the realistic simulation of STT devices. First, this model uses the macrospin approach, where the free layer is described by a single spin. While this assumption is valid for device sizes below the exchange length, another problem with this model is the retrieval of the angular dependence η that depends on the material parameters of the different layers, as well as their geometry. These dependencies are nontrivial, and thus η is usually determined in a phenomenological fashion.

In this work, we use the spin-diffusion model [14] that introduces the spin accumulation s , which describes the imbalance of magnetic spins due to the accumulation of conducting electrons. According to the spin-diffusion model, the spin torque in any magnetic layer is given as

$$\mathbf{T} = -\frac{J}{\hbar M_s} \mathbf{m} \times s, \quad (3)$$

with J being the exchange strength between itinerant electrons and magnetization. The spin accumulation s itself is computed from

$$\frac{\partial s}{\partial t} = -\nabla \cdot \mathbf{J}_s - \frac{s}{\tau_{\text{SF}}} - J \frac{s \times \mathbf{m}}{\hbar} = \mathbf{0}, \quad (4)$$

where τ_{SF} is the spin-flip relaxation time. Note that we compute the equilibrium spin accumulation s with $\partial s / \partial t = 0$ for a given magnetization which is justified by the fact that s relaxes 2 orders of magnitude faster than \mathbf{m} [15]. With this assumption, s is uniquely solved for a given magnetization \mathbf{m} and spin current \mathbf{J}_s defined by

$$\mathbf{J}_s = \beta \frac{\mu_B}{e} \mathbf{m} \otimes \mathbf{J}_e - 2D_0 \{ \nabla s - \beta \beta' \mathbf{m} \otimes [(\nabla s)^T \mathbf{m}] \}, \quad (5)$$

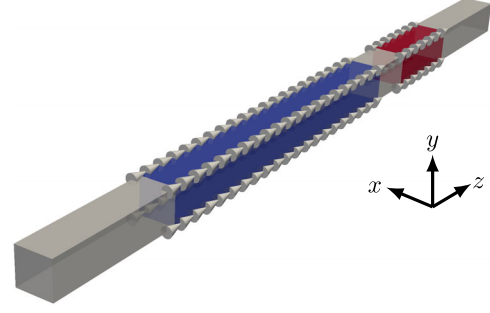


FIG. 1. The quasi-one-dimensional model with a pinned layer (blue), a free layer (red), and a spacer and leads (gray).

where \mathbf{J}_e is the electric current density, D_0 is the diffusion constant, and β and β' are dimensionless polarization parameters. Here, β is a measure of the capability of a material to polarize itinerant electrons, and β' is a measure for the sensitivity of the electric resistivity to the angle between magnetization and polarization of itinerant electrons. The numerical solution of the system (4) and (5) with the finite-element method is described in detail in Ref. [16].

In Ref. [17], we show that the averaged torque on the free-layer magnetization computed by the spin-diffusion model is well described by the model of Slonczewski, and hence both models are equivalent for system sizes below the single-domain limit. The reason for applying the spin-diffusion model in this work is the correct description of the torques on both the free layer and the pinned layer, which is crucial for the presented back-hopping mechanism.

For the investigation of the back-hopping effect, we consider a system with a pinned-layer thickness of 10 nm, a spacer-layer thickness of 1.5 nm, and a free-layer thickness of 3 nm. Additionally, the trilayer is sandwiched between two nonmagnetic leads. These leads are simulated as layers with a thickness of 4 nm. However, owing to the use of effective material parameters, the simulation results are similar to those of infinite leads [13]. The model is quasi one dimensional, i.e., the cross section of the simulated device is chosen to be a square with dimensions 1×1 nm; see Fig. 1. Since the size of a typical STT-MRAM device is considered to be below the single-domain limit, the choice of a lateral dimension is considered to be a valid assumption.

We consider out-of-plane magnetized systems in this work. In these systems, the pinned layer is mainly stabilized by a high uniaxial anisotropy. The magnetic material parameters for the pinned layer are chosen to be $\mu_0 M_s = 1.4$ T, $K_1 = 10^6$ J/m³, and $A = 10^{11}$ J/m, which is typical for FePt. For the free layer we choose material parameters $\mu_0 M_s = 1.357$ T, $K_1 = 2 \times 10^5$ J/m³, and $A = 3 \times 10^{11}$ J/m. The remaining material parameters for both magnetic layers are chosen to be $\alpha = 0.02$, $\beta = \beta' = 0.8$, $D_0 = 3 \times 10^{11}$ m²/s, $\tau_{\text{SF}} = 5 \times 10^{14}$ s, and $J = 6 \times 10^{20}$ J. The spacer layer and the leads are

simulated with material parameters similar to Ag, namely, $D_0 = 5 \times 10^{-3} \text{ m}^2/\text{s}$ and $\tau_{\text{SF}} = 10^{-12} \text{ s}$. The coordinate system is chosen such that the z axis points out of plane. In our simplified model, we consider only the exchange field and the anisotropy field as effective-field contributions. While the demagnetization field certainly has an impact on real systems by introducing shape anisotropy and interlayer coupling, it is not considered to have a qualitative impact on the results presented in this work. Moreover, omitting the demagnetization field justifies the use of the quasi-one-dimensional model since the simulation results do not depend on the lateral dimension in this case.

III. BACK-HOPPING

Figure 2 shows the current hysteresis loop for the model introduced above. The effect of back-hopping can be observed on both branches of the hysteresis loop. However, the back-hopping happens at much lower currents on the positive current branch. The initial situation is a parallel configuration of the pinned and free layers, $m_{\text{free},z} = m_{\text{pinned},z} = 1$. A positive current means that electrons are flowing from the free layer to the pinned layer. In this situation, the spin torque in the free layer is generated indirectly by electrons scattered from the pinned-layer-spacer-layer interface. After the free layer switches at a current density of $J_e = 7 \times 10^{11} \text{ A/m}^2$, the back-hopping can be observed at a current density of $J_e = 1.7 \times 10^{12} \text{ A/m}^2$ and higher. It is clear from Fig. 2 that the back-hopping of the free layer is initiated by a switching of the pinned layer.

In order to understand the perpetual switching of both layers, the spin torque acting on both layers has to be investigated in detail. For a qualitative understanding of this process, it is sufficient to consider the simplified model (2) that introduces a splitting of the overall torque into a dampinglike and a fieldlike torque. While the dampinglike torque leads to a direct relaxation of the magnetization towards the reference magnetization \mathbf{M} , the fieldlike torque leads to precessional behavior; see Fig. 3. This model can be further simplified by neglecting the fieldlike torque, as it is much smaller than the dampinglike torque in typical

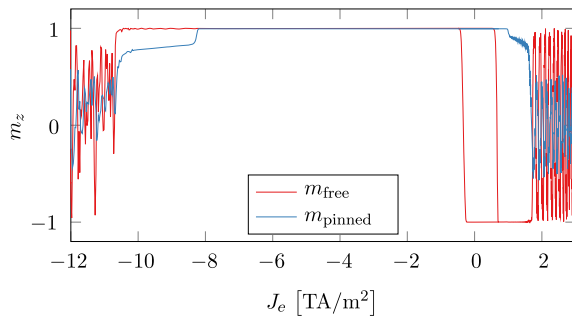


FIG. 2. Full current hysteresis loop of the presented STT-MRAM structure.

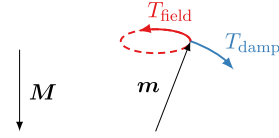


FIG. 3. Fieldlike and dampinglike torque caused by a spin-polarized current with polarization \mathbf{M} acting on the magnetization \mathbf{m} .

multilayer structures. In order to understand the switching process of the two magnetic layers above the critical current, the sign of the dampinglike torque in the different magnetic layers is decisive. A positive sign means that the magnetization seeks a parallel alignment with the reference magnetization \mathbf{M} , whereas a negative sign means that the magnetization seeks an antiparallel alignment with \mathbf{M} . Depending on \mathbf{M} , this behavior leads either to switching or stabilization of the respective layer.

The MRAM device under consideration has four different stable states in the absence of electric currents ($\uparrow\uparrow$, $\downarrow\downarrow$, $\uparrow\downarrow$, $\downarrow\uparrow$) since both the pinned and the free layer may be aligned either parallel or antiparallel with the z axis. In order to retrieve the sign of the dampinglike torque in the respective layers for these magnetization configurations from the spin-diffusion model, we apply the following procedure. We compute the spin accumulation s for the four possible configurations with the free-layer magnetization $\mathbf{m}_{\text{free}} = \pm(0, 0, 1)$ and the pinned-layer magnetization slightly tilted in the y direction $\mathbf{m}_{\text{pinned}} = \pm(0, \epsilon, 1)$ in order to avoid a collinear alignment that leads to vanishing torque. The sign of the dampinglike torque can be derived from the projection of the averaged spin accumulation s onto $\mathbf{m} \times \mathbf{M}$. In the case of the free-layer torque, the pinned-layer magnetization is taken as reference magnetization \mathbf{M} , and the sign of the dampinglike torque can be obtained by projecting s onto $\mathbf{m}_{\text{free}} \times \mathbf{m}_{\text{pinned}}$. In the case of the pinned-layer torque, the dampinglike torque can be obtained by projecting s onto $-\mathbf{m}_{\text{pinned}} \times \mathbf{m}_{\text{free}}$ taking into account a different sign of J_e . In either case, the sign of the dampinglike torque is reflected in the sign of s_x .

Figure 4(a) shows the x component of the spin accumulation s for a current J_e in the positive z direction and the four possible magnetization configurations. Performing the proposed projections reveals that, regardless of the magnetization configuration, the free layer is always subject to a negative dampinglike torque and the pinned layer is always subject to a positive dampinglike torque, which is in perfect agreement with the predictions of the Slonczewski model.

Considering these results, the switching process of the two magnetic layers at sufficiently high electric currents in the positive z direction can be understood as follows. Whenever the free and pinned layers are aligned in parallel, the spin torque stabilizes the pinned layer, while it destabilizes the free layer. This process results in the

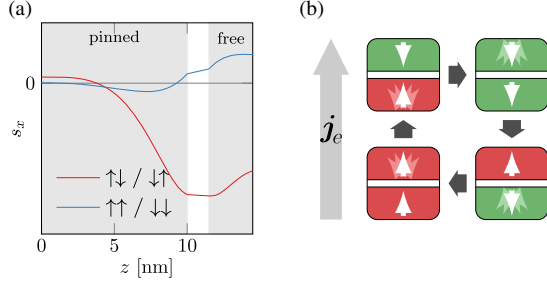


FIG. 4. Spin-accumulation and switching process of a magnetic trilayer for electric currents in the positive z direction. (a) x component of the spin accumulation for parallel and antiparallel magnetization configuration with a pinned layer slightly tilted in the y direction. (b) Cyclic switching process of the free layer (top panels) and the pinned layer (bottom panels). The direction of the electric current \mathbf{J}_e is antiparallel to the moving direction of the electrons.

switching of the free layer. For an antiparallel alignment, the free layer is stabilized, while the pinned layer switches. This behavior leads to the cyclic switching process that is depicted in Fig. 4(b).

The above explanation of the back-hopping effect assumes that the distinctive steps of the cycle happen one after another. However, simulations suggest that the switching of the two layers happens in a more dynamic fashion; see Fig. 5(a). It should be especially noted that the pinned layer never reaches saturation during the oscillation process.

The back-hopping effect as observed in Ref. [8] exhibits irregular peaks, which contradicts the oscillational behavior shown in Fig. 5(a). However, the simulation results presented so far do not account for the effect of finite temperature. In order to account for these effects, we simulate the system described above with Langevin dynamics. The effective field is complemented by a fluctuating field uncorrelated in space and time with a variance D given by

$$D = \frac{2\alpha k_B T}{\gamma \mu_0 M_s V_{\text{cell}}}, \quad (6)$$

with V_{cell} being the volume of the respective simulation cell. We solve the resulting stochastic LLG with a semi-implicit scheme [18] and a time step $h = 1$ fs. At finite temperature, back-hopping is expected to occur even below the critical current since thermal activation allows the magnetization to overcome energy barriers. Most experiments are done at room temperature. However, owing to the one-dimensional character of our model, the presented structure would not be thermally stable at 300 K. Hence, we use a temperature of $T = 20$ K in the numerical experiment, which corresponds to the temperature at which the soft magnetic part of the nanowire has a thermal stability of $11k_B T$ in order to demonstrate the qualitative influence of the temperature on the magnetization dynamics. The results for the thermally

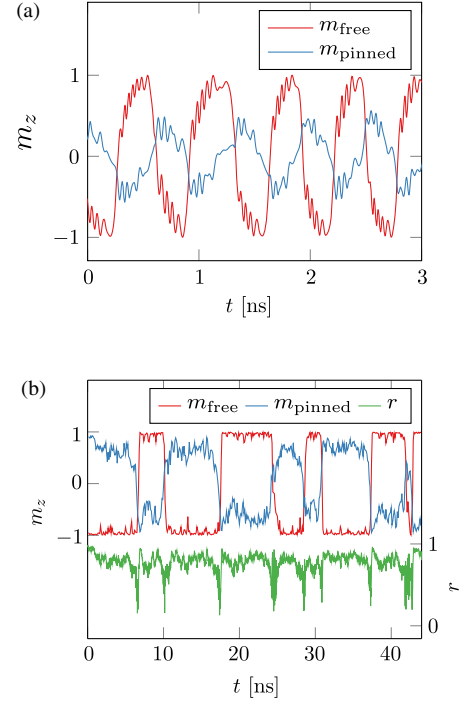


FIG. 5. Time evolution of the magnetization for electric currents in the positive z direction. (a) Deterministic simulation at $T = 0$ and $J_e = 2 \times 10^{12}$ A/m². (b) Thermally activated simulation at $T = 20$ K and $J_e = 10^{12}$ A/m². Magnetization dynamics \mathbf{m} and normalized magnetoresistance r .

activated simulation at $J_e = 1$ TA/m² are depicted in Fig. 5(b). The free-layer magnetization performs irregular switches, as observed in experiments. However, each sign change of the free-layer magnetization from -1 to 1 is initiated by a significant reduction of the pinned-layer magnetization. This result confirms the previously introduced mechanism as the origin of the back-hopping effect. The finite temperature alone does not lead to the switching of the free-layer magnetization, which is stabilized by the spin torque. Hence, the back-hopping effect is caused only by the destabilization of the pinned layer.

In experiments, the back-hopping effect is usually observed indirectly through the giant magnetoresistance (GMR) signal of the complete stack. In order to make our findings comparable to these measurements, we apply a simple GMR model to the magnetization dynamics. Namely, we assume a relative resistance r defined by

$$r(\theta) = \sin^2(\theta/2) = \frac{R(\theta) - R(0)}{R(\pi) - R(0)}, \quad (7)$$

with θ being the angle between the free-layer magnetization and the pinned-layer magnetization that is considered to give a good qualitative description of the GMR [19]. The results for this model are depicted in Fig. 5(b) along with the magnetization dynamics. The GMR signal

shows clear peaks at free-layer switching that can be explained with the switching cycle depicted in Fig. 4(b). Each free-layer switch is initiated by the switching of the pinned layer. The switching process leads to a brief moment of parallel alignment of both layers, resulting in a lower magnetoresistance.

The simulated GMR signal of the model system resembles some of the various published experimental data on back-hopping; see, e.g., Refs. [4–6,8]. However, some of the experimentally measured GMR signals exhibit considerable periods of low GMR signal, in contrast to the sharp peaks found in simulation. Possible origins for this mismatch are the assumptions and simplifications introduced by the model system. Another possible reason for these deviations is a different back-hopping mechanism in the respective experiments. This being said, this work does not attempt to give quantitative measures for back-hopping in real devices, nor does it claim that the presented mechanism is the only possible reason for back-hopping.

While the model system is perpendicularly magnetized, the same cyclic process can also be reproduced in in-plane magnetized multilayer structures. In fact, in-plane systems are expected to be more prone to back-hopping since the pinned layer in such systems is stabilized only by shape anisotropy. Perpendicular systems, on the other hand, exploit anisotropies of magnetic multilayers to stabilize the pinned layer, which enables a better control of the anisotropy strength of the pinned layer. This consideration is supported by experimental data. While different experimental studies demonstrate back-hopping for in-plane systems [5,6] as well as perpendicular systems [7,20], the effect has been considered a minor problem for perpendicular systems [21]. However, with devices shrinking in size [22], it becomes more challenging to stabilize the pinned layer [23]. Hence, back-hopping is expected to become a serious issue for perpendicular systems, too. Note that the diffusion model, which is used throughout this work, applies to metallic junctions, while modern perpendicular MRAM devices are usually magnetic tunnel junctions (MTJs). However, the back-hopping effect has also been observed in MTJs [24], and the general mechanism of the hopping process is expected to be the same for ballistic transport as for diffusive transport.

IV. COUNTERMEASURES

In order to design a reliable STT-MRAM device, it is important to prevent back-hopping since it puts the device in a nonpredictable state. Hence, the material parameters of the different layers should be chosen such that the critical current for free-layer switching is well below the critical current for pinned-layer switching. Hereafter, we present the critical currents for both free layer and pinned layers for a perpendicular system with a parallel initial magnetization configuration. This means that the critical current for the free

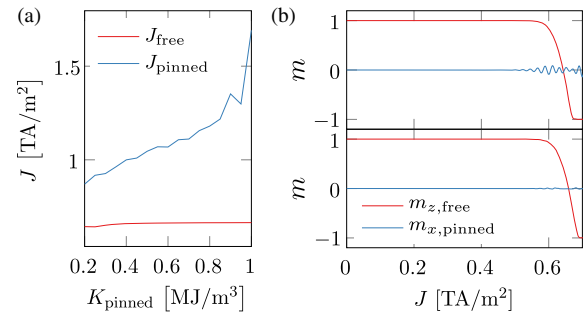


FIG. 6. Free-layer switching for different pinned-layer anisotropies. (a) Critical current densities for a switching of the free layer and the pinned layer depending on the pinned-layer anisotropy constant K_{pinned} . (b) Switching process for a linearly ramped current for $K_{\text{pinned}} = 0.2$ MJ/m³ (top) and $K_{\text{pinned}} = 0.4$ MJ/m³ (bottom).

layer indicates the switch from a parallel to an antiparallel configuration, and the critical current for the pinned layer indicates the switch back to the parallel configuration. If not stated differently, the geometry and material parameters of the system are the same as introduced previously. The critical currents are obtained by linearly increasing the current density with a rate of 0.2×10^{21} A/m² s and determining the current at switching.

Figure 6(a) shows the critical currents for different pinned-layer anisotropies. It does not come as a surprise that the free-layer critical current is almost independent from K_{pinned} , while the fixed-layer critical current increases with an increasing K_{pinned} value. However, it should be noted that the free-layer critical current shows a slight decrease of approximately 3% for very small values of K_{pinned} . This behavior can be explained by the excitation of the pinned layer which assists the switching of the free layer; see Fig. 6(b).

Another promising material parameter for critical-current manipulation is the polarization β in both the free and the pinned layer. Figure 7 shows the critical currents for different values of β_{pinned} and β_{free} . Since β is a measure of the ability of a material to polarize itinerant electrons, it is expected that a large β_{pinned} value will decrease the critical current for free-layer switching and a small β_{free} value will increase the critical current for pinned-layer switching as desired.

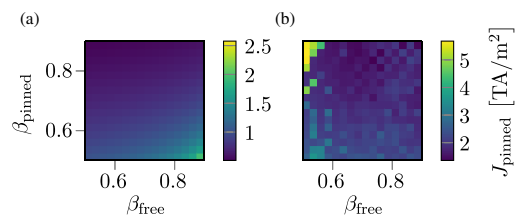


FIG. 7. Critical current densities for various polarization parameters β of the free and pinned layers. (a) Critical current for free-layer switching. (b) Critical current for pinned-layer switching.

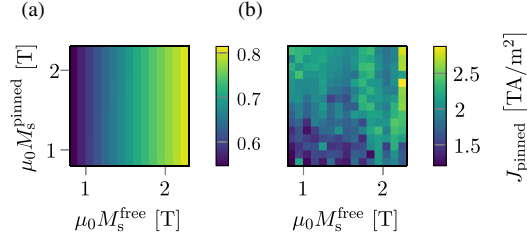


FIG. 8. Critical current densities for various saturation magnetizations M_s of the free and pinned layers. (a) Critical current for free-layer switching. (b) Critical current for pinned-layer switching.

This behavior is well reflected by the numerical experiments. Moreover, the data clearly show that a small β_{free} value decreases the critical current for free-layer switching, and also that a large β_{pinned} value increases the critical current for pinned-layer switching. This effect is not obvious when considering the switching of one layer to be initiated mainly by polarized electrons coming from the other layer. However, a highly polarizing material not only emits highly polarized electrons but also strongly depolarizes incoming electrons with a different polarization, which explains this effect well. In conclusion, materials should be chosen to have a large β_{pinned} value and a small β_{free} value in order to avoid back-hopping.

Another material parameter that is expected to influence the critical currents is the saturation magnetization M_s of the individual layers. Figure 8 shows the simulation results for varying values of M_s^{pinned} and M_s^{free} . The simulations show that the free-layer critical current J_{free} depends only on the free-layer saturation magnetization M_s^{free} ; see Fig. 8(a). The independence of J_{free} on M_s^{pinned} is well explained by the fact that the solution of the spin accumulation (4) does not depend on the saturation magnetization. However, both the spin torque (1) and the anisotropy field $H_{\text{aniso}} = 2Km_z/\mu_0 M_s$ scale with $1/M_s$. Since the critical current is a result of the competition of these two contributions, it is quite surprising that the simulated critical currents show a clear dependence on the free-layer saturation magnetization M_s^{free} . The origin of this effect, which is also found in experiments [25], is the dependence of the characteristic switching time on the saturation magnetization M_s^{free} . While, strictly speaking, the critical current remains unchanged for different values of M_s^{free} , a lower M_s^{free} value leads to faster switching. Since the critical current, as presented in Fig. 8, is determined by linearly increasing the current in time, low switching times directly lead to low critical currents. The details of this effect will be discussed elsewhere.

Note that a similar dependence should be found for the pinned-layer critical current. However, while Fig. 8(b) shows the same trend of a larger critical current for larger values of M_s^{pinned} , the simulation results are very noisy compared to Fig. 8(a). This noise can also be observed in

Fig. 7(b). The reason for the noise lies in the stiffness of the pinned layer. After the free layer switches, the spin accumulation leads to a stabilization of the free layer and a destabilization of the pinned layer. Since the pinned layer is much stiffer than the free layer, large currents are required to push the pinned layer out of its equilibrium. Moreover, the pinned layer is not instantaneously switched but tilts slightly and moves with a high frequency; see Fig. 2. In this intermediate state, the dynamics of the pinned layer generates a dynamic spin accumulation that ultimately also excites the free layer. Because of the complexity of this coupling, the critical switching current for the pinned layer is very sensitive to perturbations of the system, which leads to the observed noise in the simulation results. This noise is also expected to occur in experiments, where it might even be more significant due to the thermal effects.

V. CONCLUSION

In this paper, we investigate the back-hopping effect in perpendicularly magnetized STT-MRAM devices by means of the spin-diffusion model. Undesired switching of the pinned layer has been found to be a possible origin of the back-hopping effect, which leads to fast oscillations of the free-layer magnetization. A possible solution to avoid the switching of the pinned layer is the increase of the pinned-layer anisotropy. However, decreasing the size of MRAM devices in order to increase the storage density leads to lower anisotropies and thus increases the chances for back-hopping due to the presented mechanism.

In contrast to previous numerical studies, we apply the spin-diffusion model for the description of spin torque. Compared to the simple macrospin model by Slonczewski, this model enables an accurate description of the torque on both magnetic layers depending on various material parameters. Our numerical studies suggest that a high polarization β_{pinned} of the pinned layer and a low saturation magnetization M_s^{free} in the free layer result in a low critical current for free-layer switching. Similarly, low β_{free} and high M_s^{pinned} values result in a high critical current for pinned-layer switching, and thus back-hopping.

ACKNOWLEDGMENTS

C. A. would like to thank Kazuhiro Hono for making this collaborative work possible. The financial support from the Austrian Federal Ministry for Digital and Economic Affairs and the National Foundation for Research, Technology and Development, as well as the Austrian Science Fund (FWF) under Grant No. F4112 SFB ViCoM, the Vienna Science and Technology Fund (WWTF) under Grant No. MA14-44, Grant-in-Aids for Young Scientific Research B (17K14802), and MEXT Grant-in-Aids for Scientific Research (Grant No. 16H03853) of Japan, is gratefully acknowledged.

- [1] Y. Huai, Spin-transfer torque MRAM (STT-MRAM): Challenges and prospects, *AAPPS Bull.* **18**, 33 (2008).
- [2] C. J. Lin, S. H. Kang, Y. J. Wang, K. Lee, X. Zhu, W. C. Chen, X. Li, W. N. Hsu, Y. C. Kao, M. T. Liu, W. C. Chen, YiChing Lin, M. Nowak, N. Yu, and Luan Tran, in *Proceedings of the 2009 IEEE International Electron Devices Meeting (IEDM), Baltimore, 2009* (IEEE, New York, 2009), p. 1.
- [3] A. V. Khvalkovskiy, D. Apalkov, S. Watts, R. Chepulskii, R. S. Beach, A. Ong, X. Tang, A. Driskill-Smith, W. H. Butler, P. B. Visscher, D. Lottis, E. Chen, V. Nikitin, and M. Krounbi, Basic principles of STT-MRAM cell operation in memory arrays, *J. Phys. D* **46**, 074001 (2013).
- [4] T. Min, J. Z. Sun, R. Beach, D. Tang, and P. Wang, Back-hopping after spin torque transfer induced magnetization switching in magnetic tunnel junction cells, *J. Appl. Phys.* **105**, 07D126 (2009).
- [5] M. R. Pufall, W. H. Rippard, S. Kaka, S. E. Russek, T. J. Silva, J. Katine, and M. Carey, Large-angle, gigahertz-rate random telegraph switching induced by spin-momentum transfer, *Phys. Rev. B* **69**, 214409 (2004).
- [6] S. Urazhdin, N. O. Birge, W. P. Pratt, Jr., and J. Bass, Current-Driven Magnetic Excitations in Permalloy-Based Multilayer Nanopillars, *Phys. Rev. Lett.* **91**, 146803 (2003).
- [7] T. Devolder, J.-V. Kim, F. Garcia-Sanchez, J. Swerts, W. Kim, S. Couet, G. Kar, and A. Furnemont, Time-resolved spin-torque switching in MgO-based perpendicularly magnetized tunnel junctions, *Phys. Rev. B* **93**, 024420 (2016).
- [8] J. Z. Sun, M. C. Gaidis, G. Hu, E. J. O'Sullivan, S. L. Brown, J. J. Nowak, P. L. Trouilloud, and D. C. Worledge, High-bias backhopping in nanosecond time-domain spin-torque switches of MgO-based magnetic tunnel junctions, *J. Appl. Phys.* **105**, 07D109 (2009).
- [9] W. Skowroński, P. Ogrodnik, J. Wrona, T. Stobiecki, R. Świrkowicz, J. Barnaś, G. Reiss, and S. van Dijken, Back-hopping effect in magnetic tunnel junctions: Comparison between theory and experiment, *J. Appl. Phys.* **114**, 233905 (2013).
- [10] Z. Hou, Y. Liu, S. Cardoso, P. P. Freitas, H. Chen, and C.-R. Chang, Dynamics of the reference layer driven by spin-transfer torque: Analytical versus simulation model, *J. Appl. Phys.* **109**, 113914 (2011).
- [11] S.-M. Seo and K.-J. Lee, Current-induced synchronized switching of magnetization, *Appl. Phys. Lett.* **101**, 062408 (2012).
- [12] J. C. Slonczewski, Currents and torques in metallic magnetic multilayers, *J. Magn. Magn. Mater.* **247**, 324 (2002).
- [13] C. Abert, H. Sepelri-Amin, F. Bruckner, C. Vogler, M. Hayashi, and D. Suess, Fieldlike and Dampinglike Spin-Transfer Torque in Magnetic Multilayers, *Phys. Rev. Applied* **7**, 054007 (2017).
- [14] S. Zhang, P. M. Levy, and A. Fert, Mechanisms of Spin-Polarized Current-Driven Magnetization Switching, *Phys. Rev. Lett.* **88**, 236601 (2002).
- [15] S. Zhang and Z. Li, Roles of Nonequilibrium Conduction Electrons on the Magnetization Dynamics of Ferromagnets, *Phys. Rev. Lett.* **93**, 127204 (2004).
- [16] M. Ruggeri, C. Abert, G. Hrkac, D. Suess, and D. Praetorius, Coupling of dynamical micromagnetism and a stationary spin drift-diffusion equation: A step towards a fully self-consistent spintronics framework, *Physica (Amsterdam)* **486B**, 88 (2016).
- [17] C. Abert, M. Ruggeri, F. Bruckner, C. Vogler, G. Hrkac, D. Praetorius, and D. Suess, A three-dimensional spin-diffusion model for micromagnetics, *Sci. Rep.* **5**, 14855 (2015).
- [18] M. J. Werner and P. D. Drummond, Robust algorithms for solving stochastic partial differential equations, *J. Comput. Phys.* **132**, 312 (1997).
- [19] B. Dieny, V. S. Speriosu, S. S. P. Parkin, B. A. Gurney, D. R. Wilhoit, and D. Mauri, Giant magnetoresistive in soft ferromagnetic multilayers, *Phys. Rev. B* **43**, 1297 (1991).
- [20] W. Kim, S. Couet, J. Swerts, T. Lin, Y. Tomczak, L. Souriau, D. Tsvetanova, K. Sankaran, G. L. Donadio, D. Crotti, S. Van Beek, S. Rao, L. Goux, G. S. Kar, and A. Furnemont, Experimental observation of back-hopping with reference layer flipping by high-voltage pulse in perpendicular magnetic tunnel junctions, *IEEE Trans. Magn.* **52**, 1 (2016).
- [21] J. J. Nowak, R. P. Robertazzi, J. Z. Sun, G. Hu, D. W. Abraham, P. L. Trouilloud, S. Brown, M. C. Gaidis, E. J. O'Sullivan, W. J. Gallagher, and D. C. Worledge, Demonstration of ultralow bit error rates for spin-torque magnetic random-access memory with perpendicular magnetic anisotropy, *IEEE Magn. Lett.* **2**, 3000204 (2011).
- [22] S. Yuasa *et al.*, in *Proceedings of the 2013 IEEE International Electron Devices Meeting (IEDM), Washington, DC, 2013* (IEEE, New York, 2013), p. 3.1.1.
- [23] H. Sato, T. Yamamoto, M. Yamanouchi, S. Ikeda, S. Fukami, K. Kinoshita, F. Matsukura, N. Kasai, and H. Ohno, in *Proceedings of the 2013 IEEE International Electron Devices Meeting (IEDM), Washington, DC, 2013* (IEEE, New York, 2013), p. 3.2.1.
- [24] S.-C. Oh, S.-Y. Park, A. Manchon, M. Chshiev, J.-H. Han, H.-W. Lee, J.-E. Lee, K.-T. Nam, Y. Jo, Y.-C. Kong, B. Dieny, and K.-J. Lee, Bias-voltage dependence of perpendicular spin-transfer torque in asymmetric MgO-based magnetic tunnel junctions, *Nat. Phys.* **5**, 898 (2009).
- [25] K. Yagami, A. A. Tulapurkar, A. Fukushima, and Y. Suzuki, Low-current spin-transfer switching and its thermal durability in a low-saturation-magnetization nanomagnet, *Appl. Phys. Lett.* **85**, 5634 (2004).